

1 **Polarisability-dependent separation of lithium iron phosphate**
2 **(LFP) and graphite in dielectrophoretic filtration**

3 Mariia Kepper¹, Alica Rother², Jorg Thöming^{1, 2, 3}, Georg R. Pesch^{4*}

4 ¹ *University of Bremen, Faculty of Production Engineering, Chemical Process Engineering*
5 *(CVT), Germany*

6 ² *University of Bremen, Center for Environmental Research and Sustainable Technologies*
7 *(UFT), Germany*

8 ³ *MAPEX Center for Materials and Processes, University of Bremen, Bremen, Germany*

9 ⁴ *University College Dublin, School of Chemical and Bioprocess Engineering, Dublin, Ireland*

10 *Correspondence should be addressed to the following author(s):

11 Full name: Georg Pesch

12 Department: School of Chemical and Bioprocess Engineering

13 Institution: University College Dublin

14 Address: University College Dublin, School of Chemical and Bioprocess Engineering,
15 Belfield, Dublin, Ireland

16 Email: georg.pesch@ucd.ie

17 **Keywords:** Lithium-ion batteries, Filtration, separation, insulator-based dielectrophoresis,
18 high-throughput dielectrophoresis

19 **Abbreviations:** **LIB**, Lithium-ion batteries; **DEP**, dielectrophoresis; **LFP**, lithium iron
20 phosphate

21 **Abstract**

22 Lithium-ion batteries (LIB) are integrated in a wide range of electronic devices that are an
23 integral part of our modern world. Growing number of LIBs that reach their end of life
24 demands development of effective recycling strategies to recover rare and/or expensive
25 battery materials. Dielectrophoresis (DEP) is an electrokinetic particle manipulation
26 technique that allows for selective particle separation based on properties, such as material,
27 size, and shape. Here, we demonstrate separation of lithium iron phosphate (LFP) and
28 graphite using dielectrophoretic filtration. Graphite and LFP are two common LIB anode and
29 cathode materials. We demonstrate both: non-selective separation using pure suspensions
30 of both graphite and uncoated LFP and an isolation of graphite from a mixture of uncoated
31 LFP and graphite. We confirmed that LFP shows negative DEP while graphite shows positive
32 DEP. We determined the conductivity at which material-selective polarisability-based
33 separation becomes possible, thus, proofing the concept of sorting of non-carbon coated
34 lithium iron phosphate (LiFePO_4) and graphite. These results reinforce one possibility of using
35 DEP filtration as a potential method for direct physical recycling of battery material waste.

36 **1. Introduction**

37 Lithium-ion batteries (LIBs) are used in many electronic devices that surround our everyday
38 life. The constantly growing number of LIBs that reach their end of life demands development
39 of an appropriate recycling procedure. Cathode active materials are usually lithium metal
40 oxides while the anode active material is graphite. Demand of graphite in the context of LIB
41 production is 10-20 times higher than that of lithium [1]. To reduce dependence on natural or
42 synthetic virgin graphite, proper recycling methods for this material are essential [1]. The
43 most common methods for LIB recycling are pyrometallurgy, hydrometallurgy, and direct
44 physical [2]. Pyrometallurgy does not require any pre-treatment but suffers from large energy

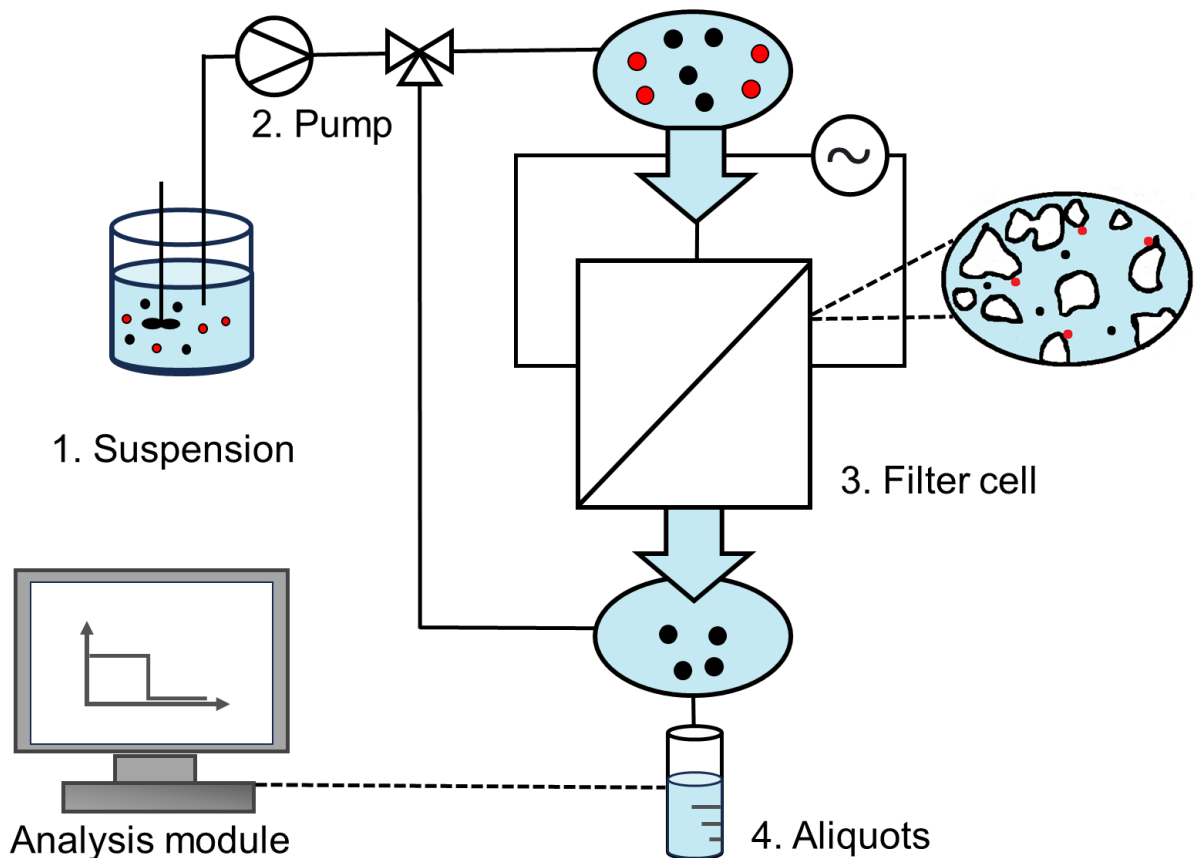
45 needs and can cause environmental pollution with toxic gases that are produced during the
46 process. Additionally, for a full recovery, pyrometallurgy must always be followed by a
47 hydrometallurgical step to treat the alloy [3]. Hydrometallurgy involves huge consumption of
48 chemical reagents [2]. Both hydrometallurgy and pyrometallurgy focus only on the recovery
49 of the main cathode components, graphite is lost in both processes. Direct physical recycling
50 processes focus on using particle technology to directly separate and recover the cathode
51 and anode active material, however, universally applicable methods to achieve this task are
52 lacking.

53 Here, we research dielectrophoresis (DEP) as a method to separate cathode and anode
54 material. DEP allows for a particle separation based on polarisability. Our group developed
55 several approaches to treat particle systems at high throughput using DEP [4–6]. Here, we
56 are expanding the scope of dielectrophoretic filtration towards polarisability-dependent
57 separation of LIB materials of different conductivities. Dielectrophoretic filtration [5,7-11] is a
58 macroscopic high-throughput DEP method based on applying an electric field across a
59 porous dielectric material (filter). This filter disturbs the electric field, creating local field
60 extrema which can be used to selectively trap particles by dielectrophoresis. The
61 dielectrophoretic force is proportional to the electric field strength and linearly dependent on
62 the Clausius-Mossotti (CM) factor [12]. The CM factor is influenced by the complex
63 permittivities of the particle and the medium in which the particle is submerged. At low
64 frequencies, the CM factor depends only on the medium and particle conductivities.
65 Therefore, DEP can be used for material-selective separation by controlling and tuning the
66 conductivity of the suspension medium. When medium conductivity becomes significantly
67 higher than the conductivity of the target particles, the particles are getting pushed away
68 from electric field maxima, they are said to experience negative dielectrophoresis (nDEP).

69 When the medium conductivity is lower than the particle conductivity, then the particles are
70 attracted towards the local field maxima, they are said to experience positive DEP (pDEP).
71 Particles that experience pDEP will become immobilized in local field maxima in the filter and
72 we can use DEP filtration to selectively trap target particles. It is possible to recover the
73 trapped particles by switching off the electric field. In another work from our group, graphite
74 particles were isolated from significantly smaller carbon black-coated LFP particles (i.e.,
75 conductive particles) through pDEP using electrode-based dielectrophoresis [6]. While both
76 particles showed pDEP, separation was possible because the DEP force is volume
77 dependent. Here, we show that graphite particles can be isolated from uncoated, i.e., non-
78 conductive, LFP particles of comparable size using dielectrophoretic filtration. Thus, we show
79 polarisability-dependent sorting of particles. We show that we can separate graphite powder
80 from a mixture of graphite and uncoated lithium-iron phosphate powder in aqueous
81 suspension. While this study aims to expand the scope of DEP filtration, we also pave the
82 way towards solving an important problem in the recycling of LIB, i.e., the selective recovery of
83 graphite from LIB waste.

84 **2. Material and Methods**

85 The main components of our setup are the particle suspension, filter cell and analysis module
86 (Fig. 1).

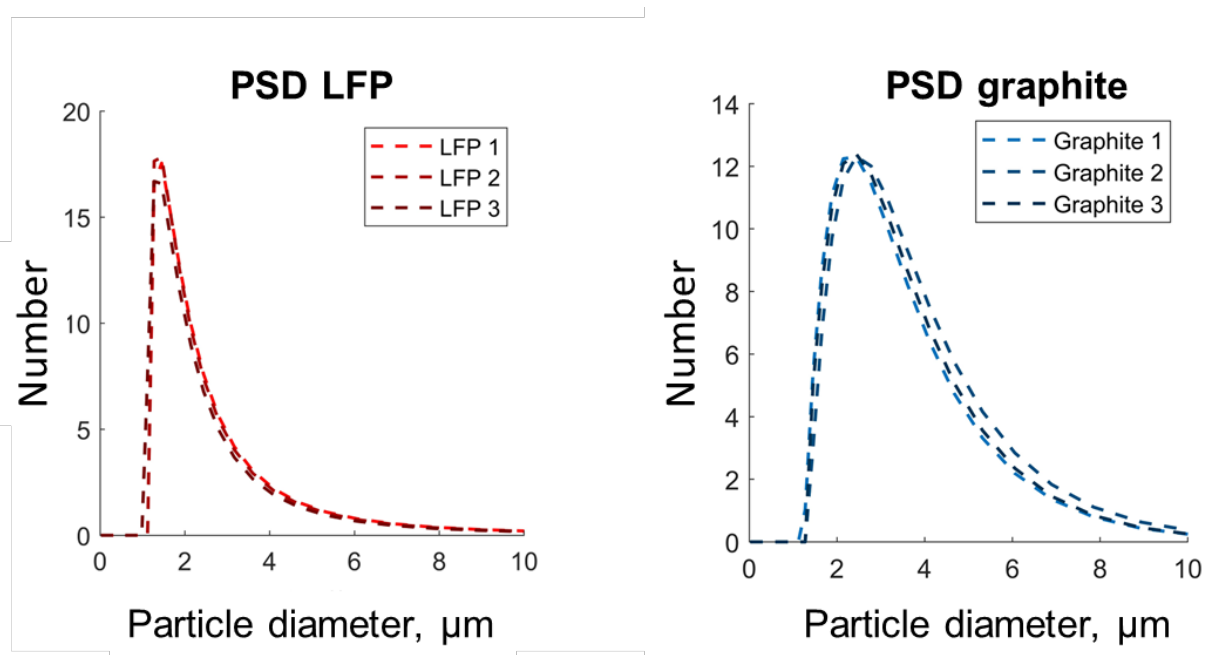


87

88 **Figure 1.** DEP filtration, a schematic setup of the filtration experiment.

89 The core of the setup, the DEP filter unit, is identical to the one used in Ref. [7, 9]. The filter
 90 cell has dimensions of $8 \times 29 \times 18 \text{ mm}^3$ and is made of polytetrafluoroethylene. Here, we are
 91 using a packed bed filter of grained silica material (sand) as filter matrix. The matrix is
 92 characterized in detail in Ref. [7]. The pores of the filter are ≥ 20 times larger than the size
 93 of the investigated particles. Two macroscopic electrodes, made of the stainless steel, are
 94 mounted inside the filter cell region at a distance of 8 mm. An ac electric field was applied
 95 across these electrodes. The signal was generated by a function generator (HM8131,
 96 Hameg Instruments GmbH, Germany) and amplified by a voltage amplifier (PZD700A, TREK
 97 Inc., USA). The resulted voltage on the setup was measured using the power analyser
 98 LMG670 (ZES ZIMMER ElectronicSystems GmbH, Germany). The suspension was
 99 delivered to the filter cell with a peristaltic pump (REGLO Analog, Ismatec, Switzerland).

100 During all the experiments, the flow rate was constant and kept at 360 mL/h. The connecting
101 tubes are accompanied with a three-way valve, allowing for the suspension to go either via
102 the filter cell to the analysis module, or via the bypass to the analysis module.



103

104 **Figure 2.** Particle size distribution (PSD), number-based and additionally normalized
105 distribution of two particle systems (LFP and graphite), measured three times each with laser
106 diffraction.

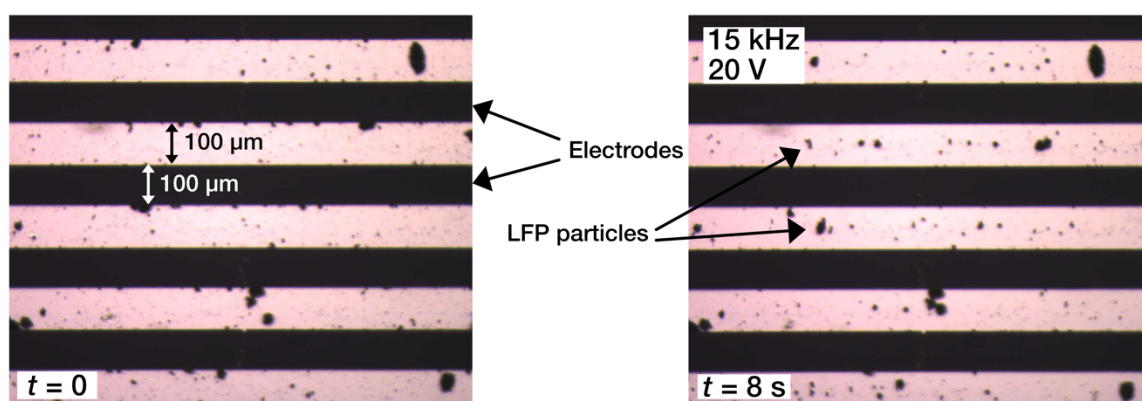
107 Particle suspensions were uncoated lithium iron phosphate (LFP) and graphite. Virgin
108 material was purchased commercially in the form of the fine powders with particle size less
109 than 5 μm (company information) from Sigma-Aldrich. Graphite (TIMCAL KS-6) was
110 purchased as powder with mean particle size ≤ 3.4 μm (company information) from MSE
111 Supplies. Before experimentation, we additionally measured the particle size distributions
112 using laser diffraction (LD, Mastersizer 2000, Malvern Panalytical GmbH, United Kingdom),
113 see Fig. 2 (more details are in supplementary materials), and found that the results fall close
114 into the size range given by the companies. Pure particle suspensions were prepared by
115 suspending particle in pure deionized water (Omniatap 6 UV/UF, Starkpure GmbH,
116 Germany) to a concentration 4 mg/L (graphite) and 8 mg/L (LFP). We further added Tween

117 20 solution (Sigma-Aldrich, Germany) to a final concentration of 0.004% vol. The conductivity
118 of the final suspension was tuned by adding 0.1 M KCl to a final value of 1–15 $\mu\text{S}/\text{cm}$.
119 Through the experimental stage, the suspension was always disturbed with a stirring
120 magnet. For the preparation of the mixture suspension, graphite and LFP were mixed into
121 one beaker in the same concentrations as they were in separate suspensions before.
122 The trapping efficiency of the separate mixtures was qualitatively measured using a
123 spectrometer (HORIBA, FluorMAX-4) on-line reflection measurement combined with
124 MATLAB processing [7, 13]. The suspension was flowing through a quartz cuvette (176.762-
125 QS, Hellma). A qualitative estimate of (non-selective) separation efficiency is given by on-
126 line measuring the reflection of the particles at the outlet of the setup. The particles are not
127 ideal spheres (supplier information) so that we can only qualitatively measure their
128 concentration like this. The processing of the signal was done similar to our previous work,
129 by the use of the MATLAB script from the previous study, which calculates the trapping
130 efficiency by subtracting from 100 % a ratio of the signal from the particles going freely to the
131 filter, to the signal of the particles, recorded while the electric field was on [7, 13].
132 To address quantitatively the separation efficiency of LFP in a mixture with graphite, we used
133 atomic absorption spectroscopy (AAS). For AAS, we collected a defined volume of around
134 20 mL of the suspension into 50 mL volumetric flasks during the different stages of the
135 experiment. The LFP was dissolved by adding 3 mL 65 % nitric acid (VWR International,
136 Belgium) and 3 mL 30 % hydrogen peroxide (Sigma-Aldrich, Germany). After the volumetric
137 flasks were topped up with pure deionized water, the lithium content inside the prepared
138 mixture was determine with AAS using a Solaar 989 QZ AA Spectrometer (Unicam, England)
139 with a GF90+ furnace and an FS90+ autosampler.

140 3. Results and Discussion

141 The graphite particles have a significantly higher bulk conductivity value than the aqueous
142 suspension and we expect them to show pDEP behaviour. The uncoated LFP particles,
143 however, have a low conductivity value of around 10^{-7} – 10^{-8} S/cm, which is lower than that of
144 the medium and they should therefore demonstrate nDEP behaviour [14, 15].

145 We have firstly investigated if LFP indeed shows negative DEP in a simple setup. A 50 μ L
146 drop of the LFP suspension at 30 μ S/cm conductivity was placed on top of an interdigitated
147 electrode array and we directly observed particle movement using a microscope. For this, a
148 voltage of 20 V_{RMS} at 15 kHz was applied with a signal generator (Rigol DG4062, Rigol
149 Technologies EU GmbH, Puchheim, Germany). The particle movement was recorded using
150 an inverted microscope (ECLIPSE Ts2R-FL, Nikon Instruments Europe BV, Amsterdam,
151 Netherlands) and a CMOS camera (Grasshopper GS3-U3-51S5C-C, FLIR Systems Inc.,
152 Wilsonville, OR, USA). The interdigitated electrodes have an arm width and gap width of 100
153 μ m and were fabricated using standard cleanroom techniques. Upon application of the
154 voltage, LFP particles indeed accumulated in the space between the electrodes, which is
155 typical behaviour for particles that show nDEP (see Fig. 3 and the video in the supplement).

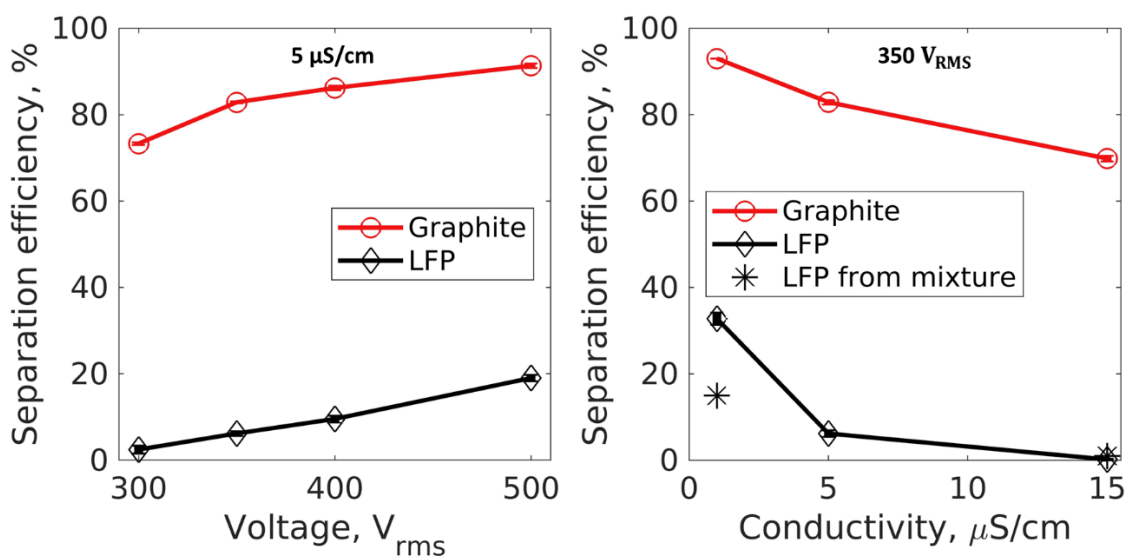


156

157 **Figure 3.** Behaviour of LFP (black particles) in an array of interdigitated electrodes at 20 V
158 and 15 kHz and at a conductivity of 30 μ S/cm. Upon application of an electric field, the

159 randomly distributed LFP particles (left) are predominantly repelled to the space between the
160 electrodes (right). This is typical behaviour for particles that experience nDEP. Electrode
161 distance is 100 μm .

162 We then performed LFP and graphite separation experiments with our filter cell setup. In
163 individual (non-selective) experiments, at 5 $\mu\text{S}/\text{cm}$, the trapping of both graphite increases
164 with voltage, as expected from the DEP theory for pDEP particles (Fig. 4, left). The trapping
165 of LFP also increases with voltage, which might be due to nDEP retention, as we have
166 previously observed [9].



167

168 **Figure 4.** DEP trapping efficiency of two separate powders, analysed with the reflection
169 measurement and an additional result of trapping of only LFP from the mixture (*) at 15 kHz,
170 360 mL/h flow rate. Left: Dependence on the voltage (at 5 $\mu\text{S}/\text{cm}$ conductivity); right:
171 dependence on the conductivity (at 350 V_{RMS} voltage) with their respective standard
172 deviations from three repetitions.

173 While at 300 V_{rms} , LFP shows almost no trapping, it does show appreciable separation of
174 almost 20 % at 500 V_{rms} . Further, we observed that LFP trapping decreases with increasing

175 solution conductivity (Fig. 4, right). While at 1 $\mu\text{S}/\text{cm}$ and 350 V_{rms} , LFP shows trapping above
176 30 %, it drops to 1% at 15 $\mu\text{S}/\text{cm}$. Graphite trapping efficiency also drops slightly with
177 increasing conductivity, from 90% at 1 $\mu\text{S}/\text{cm}$ to 70% at 15 $\mu\text{S}/\text{cm}$. Thus, at 15 $\mu\text{S}/\text{cm}$, LFP
178 trapping is negligible while graphite trapping is high. The mechanism why LFP shows higher
179 trapping at lower conductivities is unclear. Its bulk conductivity value should be well below 1
180 $\mu\text{S}/\text{cm}$ and from microscopy experiments, we know that LFP shows nDEP at 30 $\mu\text{S}/\text{cm}$. We
181 could not perform microscopy experiments at lower conductivities, as the required particle
182 load was too high to achieve lower conductivities. The small decline of the trapping efficiency
183 for graphite is believed to be associated with thermal effects at the higher conductivities of
184 aqueous suspension. Such an explanation was given for a similar observation with
185 polystyrene particles, assuming that an increase in conductivity raises temperature due to
186 more energy dissipation and this in turn increases a natural convection of the fluid creating
187 more “undirected” fluid motion [9].

188 To separate graphite from a mixture of graphite and LFP of similar size, both particles were
189 added in one suspension. The trapping efficiency of LFP was evaluated at 15 kHz, 350 V_{rms}
190 using the AAS protocol at two solution conductivities, 1 and 15 $\mu\text{S}/\text{cm}$, respectively. The
191 trapping efficiency of LFP in these experiments is plotted as stars in Fig. 4. Similar to the
192 pure particle experiments, LFP showed a trapping efficiency of roughly 1 % at 15 $\mu\text{S}/\text{cm}$ and
193 of 15 % at 1 $\mu\text{S}/\text{cm}$. The difference between trapping efficiency in pure particle and mixture
194 experiments (i.e., black dots vs. black stars in the right Fig. 4) is probably because two
195 different measurement techniques were used. As mentioned, reflection measurement can
196 only give a qualitative estimate of separation, while AAS actually measures lithium content
197 and gives more precise results, as also observed before [6]. We did not measure the graphite

198 concentration in mixture experiments and thus assume that graphite shows a separation
199 efficiency similar to pure particle experiments.

200 **4. Conclusions**

201 Our research indicates the potential of dielectrophoretic filtration as an additional purification
202 step for recycling of battery materials. Our findings demonstrate that by manipulation of the
203 conductivity of the liquid medium, we can selectively separate graphite from a mixture of
204 graphite and uncoated LFP using DEP filtration. This is based on differences in the
205 polarisability of both particles. Additional research is required to further estimate the
206 technique in use. Especially, it is essential to evaluate the proper recovery rate of the target
207 particles and to tune the filter matrix geometrical parameters to avoid unwanted nDEP
208 trapping of non-target particles. It's important to note that while we successfully separated
209 commercially available particles, the application to real black mass with graphite-coated LFP
210 poses additional challenges.

211 **Acknowledgements**

212 The authors would like to thank Jasper Giesler, Laura Weirauch, Swantje Drolshagen
213 (University of Bremen) and Askar Kvaratsheliya (Leibniz Institute for Materials Engineering,
214 IWT) for their assistance.

215

216 **Author contributions**

217 **Mariia Kepper:** conceptualization, project administration, methodology, investigation,
218 validation, visualization, formal analysis, writing – original draft, review & editing. **Alica**

219 **Rother**: investigation (AAS), data curation, formal analysis (AAS). **Jorg Thöming**:
220 methodology, resources, review & editing. **Georg Pesch**: conceptualization, project
221 administration, methodology, validation, supervision, writing - review & editing.

222 **Data Availability**

223 An online repository (referred as supplementary materials in this text) is accompanying this
224 article and contains of details on the evaluation of DEP data, additional details on the
225 measurement of the particle-size distribution data of the LFP and graphite, notes on AAS
226 analysis and a video demonstrating nDEP of LFP [13]. Additional information is available
227 from the corresponding author upon a reasonable request.

228 **Conflict of interest**

229 The authors declare no competing interests.

230 **5. References**

- 231 [1] Natarajan S, Aravindan V. An Urgent Call to Spent LIB Recycling: Whys and
232 Wherefores for Graphite Recovery. *Adv Energy Mater* 2020; 10: 2002238.
- 233 [2] Al-Shammari H, Farhad S. Chapter 13 - Separating battery nano/microelectrode
234 active materials with the physical method. In: Farhad S, Gupta RK, Yasin G, Nguyen
235 Remanufacturing, and Reusing TABT-NT for BR (eds). *Micro and Nano*
236 *Technologies*. Elsevier, 2022, pp 263–286.
- 237 [3] Windisch-Kern S, Gerold E, Nigl T, Jandric A, Altendorfer M, Rutrecht B et al.
238 Recycling chains for lithium-ion batteries: A critical examination of current

- 239 challenges, opportunities and process dependencies. *Waste Manag* 2022; 138: 125–
240 139.
- 241 [4] Giesler J, Weirauch L, Thöming J, Baune M, Pesch GR. Separating microparticles by
242 material and size using dielectrophoretic chromatography with frequency
243 modulation. *Sci Rep* 2021; 11: 16861.
- 244 [5] Weirauch L, Giesler J, Baune M, Pesch GR, Thöming J. Shape-selective
245 remobilization of microparticles in a mesh-based DEP filter at high throughput. *Sep*
246 *Purif Technol* 2022; 300: 121792.
- 247 [6] Giesler J, Weirauch L, Rother A, Thöming J, Pesch GR, Baune M. Sorting Lithium-
248 Ion Battery Electrode Materials Using Dielectrophoresis. *ACS Omega* 2023; 8:
249 26635–26643.
- 250 [7] Kepper M, Karim MN, Baune M, Thöming J, Pesch GR. Influence of the filter grain
251 morphology on separation efficiency in dielectrophoretic filtration. *Electrophoresis*.
252 2023; 1–10.
- 253 [8] Pesch GR, Lorenz M, Sachdev S, Salameh S, Du F, Baune M et al. Bridging the
254 scales in high-throughput dielectrophoretic (bio-)particle separation in porous media.
255 *Sci Rep* 2018; 8: 10480.
- 256 [9] Lorenz M, Malangré D, Du F, Baune M, Thöming J, Pesch GR. High-throughput
257 dielectrophoretic filtration of sub-micron and micro particles in macroscopic porous
258 materials. *Anal Bioanal Chem* 2020; 412: 3903–3914.
- 259 [10] Weirauch L, Lorenz M, Hill N, Lapizco-Encinas BH, Baune M, Pesch GR
260 et al. Material-selective separation of mixed microparticles via insulator-based
261 dielectrophoresis. *Biomicrofluidics*. 2019; 13:64112.
- 262 [11] Zhou G, Imamura M, Suehiro J, Hara M. A dielectrophoretic filter for separation and

- 263 collection of fine particles suspended in liquid. In: Conference record of the 2002
264 IEEE industry applications conference. 37th IAS annual meeting (Cat.
265 No.02CH37344). Vol. 2. Pittsburgh, PA, USA: IEEE; 2002. pp. 1404–11.
- 266 [12] Pohl HA. The Motion and Precipitation of Suspensoids in Divergent Electric Fields. J
267 Appl Phys 1951; 22: 869–871.
- 268 [13] Kepper M, Rother A. Online repository for "Polarisability-dependent separation of
269 lithium iron phosphate (LFP) and graphite in dielectrophoretic filtration". Zenodo.2023,
270 <https://doi.org/10.5281/zenodo.10120331>.
- 271 [14] Yang M-R, Ke W, Wu S. Improving electrochemical properties of lithium iron
272 phosphate by addition of vanadium. J Power Sources 2007; 165: 646–650.
- 273 [15] Wang GX, Bewlay SL, Konstantinov K, Liu HK, Dou SX, Ahn J-H. Physical and
274 electrochemical properties of doped lithium iron phosphate electrodes. Electrochim
275 Acta 2004; 50: 443–447.